Available online at www.sciencedirect.com
ScienceDirect
Trans. Nonferrous Met. Soc. China 28(2018) 794−801
Transactions of Nonferrous Metals Society of China
www.tnmsc.cn

Adsorption of Cd^{2+} in aqueous solutions using $KMnO_4$-modified activated carbon derived from *Astragalus* residue

Ning-chuan FENG[1], Wei FAN[1], Mei-lin ZHU[1], Xue-yi GUO[2]

1. School of Basic Medical Science, Ningxia Medical University, Yinchuan 750004, China;
2. School of Metallurgy and Environment, Central South University, Changsha 410083, China

Received 19 October 2016; accepted 26 October 2017

Abstract: Activated carbon obtained from *Astragalus* residue was chemically activated by KOH and modified with $KMnO_4$. The samples were characterized by N_2 adsorption, Fourier transform infrared spectroscopy, X-ray diffractometry, scanning electron microscopy, and Boehm titration. Accordingly, the original and modified carbon materials were used for the removal of Cd^{2+} from aqueous solution by batch adsorption experiments. Results showed that the contents of oxygen-containing functional groups increased, and MnO_2 was nearly uniformly deposited on the surface of activated carbon after modification by $KMnO_4$. The adsorption kinetics was described by pseudo-second order model. Langmuir model fitted the adsorption-isotherm experimental data of Cd^{2+} better than the Freundlich model. The maximum adsorption capacities of the activated carbon before and after modification for Cd^{2+} were 116.96 and 217.00 mg/g, respectively. $KMnO_4$ considerably changed the physicochemical properties and surface texture of activated carbon and enhanced the adsorption capacity of activated carbon for Cd^{2+}.
Key words: *Astragalus* residue; activated carbon; modification; adsorption; Cd^{2+}

1 Introduction

Cadmium (Cd^{2+}) is one of the most commonly used heavy metals and widely utilized in industries, such as electroplating, paint pigments, plastics manufacturing, and mining [1]. Cd^{2+} is toxic even at extremely low concentrations and has been classified as a human carcinogen by the US National Toxicology Program [2]. At present, ion-exchange [3] and chemical precipitation [4] are among the treatments for Cd^{2+} removal from aqueous media. Additionally, activated carbon adsorption is used for the removal of various heavy metal ions dissolved in aqueous media. In most cases, activated carbon (AC) is synthesized from natural precursors such as coal, wood or nutshells [5,6]. Although these materials are very effective, their widespread use is restricted because of their high costs. Carbon adsorption removes organic compounds but is ineffective on removing metals and inorganic pollutants [7]. In recent years, many researchers have focused on finding economical and available materials for the preparation of activated carbon, especially from plant biomass and biomaterial waste, such as olive stone waste residue [8], and grape bagasse [9]. Activated carbon modification is gaining prominence because of the increasing need to improve the affinity of activated carbon for certain contaminants for their effective removal. Among the current modification techniques, chemical oxidation is the most commonly used owing to its simplicity, low cost, low energy requirement. Additionally, oxygen-containing functional groups can be introduced on activated carbon surfaces through this method. SONG et al [10] used HNO_3 and H_2O_2 as oxidants for modifying activated carbon and investigated the effect of liquid-phase oxidation on the Pb^{2+} adsorption capacity of activated carbon. Meanwhile, WANG et al [11] applied $KMnO_4$-modified activated carbon for Pb(II) adsorption. The results showed that chemical oxidation can be performed for enhancing the adsorption capacity of activated carbon for small molecules and ions.

Astragalus contains polysaccharides, organic acids, alkaloids, saponins and so on [12], and is commonly used in traditional Chinese medicine. After the main

Foundation item: Project supported by West China Top Discipline Program in Basic Medicine Sciences, Ningxia Medical University, China; Project (21266026) supported by the National Natural Science Foundation of China
Corresponding author: Xue-yi GUO; Tel: +86-731-88877863; E-mail: xyguo@csu.edu.cn
DOI: 10.1016/S1003-6326(18)64712-0

components of this plant are extracted, a large amount of residue, which has no economic value, is generated annually and discarded in the environment, thereby increasing solid waste; in particular, *Astragalus* residues are disposed in land fillings or incinerated and are thus a source of secondary pollution [13]. Thus, managing *Astragalus* residue is of great importance. In recent years, *Astragalus* residue has been used as feed, fertilizer, and substrate of solid-state fermentation. Notably, preparation of activated carbon through the chemical activation of *Astragalus* residue with KOH has not been reported yet. In the present work, activated carbon was prepared from *Astragalus* residue, and the obtained activated carbon was modified by $KMnO_4$. The original and modified activated carbons were both applied for the adsorption of Cd^{2+} in aqueous media.

2 Experimental

2.1 Solution preparation

Double distilled water was used to prepare all solutions, and all reagents were of analytical grade. Stock solutions of Cd^{2+} at concentrations of 1 g/L were prepared using cadmium nitrate.

2.2 Preparation of activated carbon

Astragalus residue obtained from a local pharmaceutical company in Ningxia, China was used as raw material for the preparation of AC by KOH activation. The residues were pulverized, sieved to particle size (40 mesh), washed with distilled water, and air-dried. Then, 20% (mass fraction) KOH solution was mixed with *Astragalus* residue at a ratio of 1:3 (residue:KOH, g/mL). The resulting chemical-loaded sample was then heated in a muffle furnace and activated at 600 °C for 80 min. The product was cooled to room temperature, soaked with 0.1 mol/L HCl to remove the residual KOH, and washed sequentially several times with distilled water until its filtrate reached neutral pH. The resulting activated carbon material was dried at 80 °C for 12 h and stored for subsequent use (designed as AC).

2.3 $KMnO_4$ modification of AC

Activated carbon was treated with $KMnO_4$ through dipping and heating methods. Activated carbon was placed into 0.15 mol/L $KMnO_4$ solution at a ratio of 10:1 (activated carbon:$KMnO_4$ solution, g/L) for 90 min at boiling temperature. The modification was conducted under stirring in a flask equipped with a stirrer and a reflux condenser and was heated in a thermostat water bath. Before being dried at 80 °C for 12 h, the modified activated carbon was washed repeatedly with distilled water until the effluent water was neutral. After treatment, the sample was cooled to room temperature and stored in a desiccator for later use (designed as AC-Mn).

2.4 Characterization methods

The surface areas and pore characteristics of the prepared carbons were determined by N_2 adsorption/desorption isotherm at 77 K (Micrometritics, ASAP2020). The surface morphology was observed by scanning electron microscopy (SEM, HITACHI S−3400N). X-ray diffraction (XRD, Shimadzu XRD−6000) patterns were collected by using Cu K_α radiation. The chemical structure of the carbon was qualitatively evaluated with Fourier transform infrared (FTIR) spectrometer (Nicolet, NEXUS670). The Boehm titration method [14] was performed for the qualitative and quantitative identification of the surface functional groups of the activated carbon.

2.5 Batch experiments

Batch adsorption experiments were carried out at 25 °C by agitating 0.060 g of adsorbent with 30 mL Cd^{2+} solution of desired concentration in 100 mL sealed conical flask. A shaking thermostat machine was used at a speed of 100 r/min for 2 h except for the contact time experiments. The effect of solution pH on the equilibrium adsorption of Cd^{2+} was investigated by mixing 0.060 g adsorbent with 30 mL of 100 mg/L Cd^{2+} solution between pH 3.0 and 7.0. Time variations in the range of 2−120 min were used to study the kinetics of the Cd^{2+} adsorption. In the isotherm experiments, 0.060 g adsorbent was added in 30 mL Cd^{2+} solution with Cd^{2+} solution concentration varying from 100 to 800 mg/L at the optimum pH. Once the preset contact time (2 h) was reached, the samples were filtered through a 0.45 μm filter paper. The concentration of Cd^{2+} in the solution was measured by flame atomic absorption spectrometry (Persee A_3 Atomic Absorption Spectrophotometer).

The adsorption capacity, q (mg/g), and removal rate, E (%), of Cd^{2+} at equilibrium were calculated as follows:

$$q = \frac{(\rho_0 - \rho_e)V}{m} \tag{1}$$

$$E = \frac{\rho_0 - \rho_e}{\rho_0} \times 100\% \tag{2}$$

where ρ_0 and ρ_e are the initial and equilibrium Cd^{2+} ion concentrations (mg/L) in the solutions, respectively, V is the volume of solution (L), and m is the mass of adsorbent (g).

3 Results and discussion

3.1 Characterization of adsorbents

The results of the pore structural characterization of

AC and AC-Mn are given in Table 1. AC had a large BET surface area and mostly contained micropores. The presence of micropores enhances the adsorption capacity of AC, especially for small molecules or ions such as Cd^{2+} [15]. $KMnO_4$ treatment caused the decreases in the BET surface area, total pore volume, and micropore surface area. For the initial AC, the BET surface area was 1519.53 m^2/g, which decreased to 774.13 m^2/g after modification. Total pore volume and micropore surface area changed significantly. The results indicated that the pore structure of the AC-Mn was destroyed by $KMnO_4$ through strong oxidation at a high temperature.

The physical properties of samples are summarized in Table 1. The amount of iodine (1325.17 mg/g) and that of methylene blue (139.45 mg/g) in AC were higher than those of AC-Mn (994.66 mg/g and 95.68 mg/g, respectively). The iodine number was a measure of micropore content of the activated carbon by adsorption of iodine from solutions [16]. In the present work, the iodine contents of AC and AC-Mn indicated that they are micropore-type activated carbon and thus suitable for the adsorption of small molecules and ions such as Cd^{2+}. This finding corresponded to the result of micropore surface area. The Boehm titration results of AC and AC-Mn are given in Table 1. The number of oxygen-containing functional groups, such as carboxylic and lactone groups, increased after the activated carbon was subjected to oxidation modification by $KMnO_4$. The interactions between the oxygen-containing functional groups and heavy metal ions are strong, indicating that the absorption of heavy metals by activated carbon occurs at its oxygen-containing functional groups [17]. Thus, the functional groups facilitate the adsorption of heavy metal ions.

Table 1 Some properties of activated carbons

Property	AC	AC-Mn
BET surface area/($m^2 \cdot g^{-1}$)	1519.53	774.13
Total pore volume/($cm^3 \cdot g^{-1}$)	1.04	0.66
Micropore surface area/($m^2 \cdot g^{-1}$)	1386.53	596.59
Iodine content/($mg \cdot g^{-1}$)	1325.17	994.66
Methylene blue content/($mg \cdot g^{-1}$)	139.45	95.68
Content of lactonic groups/($mmol \cdot g^{-1}$)	0.23	1.57
Content of phenolic hydroxyl groups/($mmol \cdot g^{-1}$)	1.07	0.94
Content of carboxylic acid groups/($mmol \cdot g^{-1}$)	0.42	2.82

The SEM images of AC and AC-Mn are shown in Fig. 1. The surface morphology of AC was different from that of AC-Mn. The surface of AC showed a honeycomb-like and well-developed porous structure. After AC was treated with $KMnO_4$, its surface morphology was completely changed. Conversely, the grainy structure reflected on AC-Mn in Fig. 1(b) revealed that MnO_2 was nearly uniformly deposited on the surface because of redox reactions facilitated by the impregnation of $KMnO_4$.

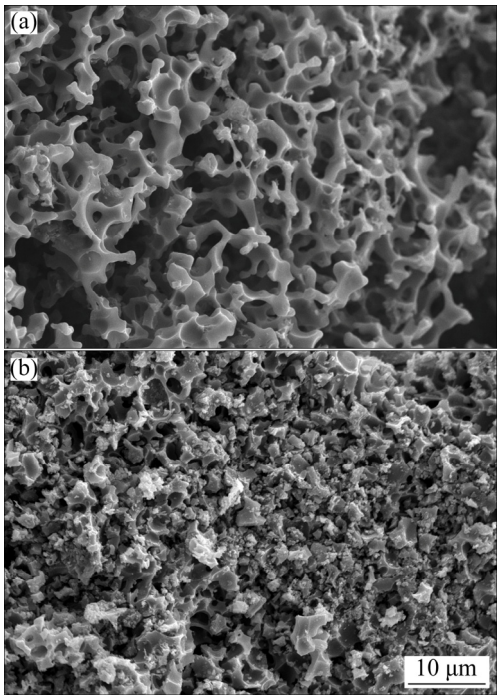

Fig. 1 SEM images of AC (a) and AC-Mn (b)

The XRD spectra of AC and AC-Mn are presented in Fig. 2. The diffraction spectrum of AC (Fig. 2(a)) displayed two diffraction peaks around 26° and 43°, corresponding to the 002 and 100 diffraction planes of graphite [18,19]. The 002 plane presented a narrow peak with steep rise, and the 100 plane displayed a broad small diffraction peak. These characteristics indicated that AC had a predominantly amorphous carbon structure. The diffraction spectrum of AC-Mn is shown in Fig. 2(b). The 002 plane showed peaks with gradually decreased intensity, whereas the 100 plane disappeared. Both results indicated that the aligned structural domains in the carbon matrix had been destroyed in the process of oxidation–reduction. Meanwhile, the extent of graphitization was decreased [19]. However, for the AC-Mn samples, the diffraction peaks at 25.91, 37.13, 42.57 and 65.95 showed the presence of MnO_2 [11,20]. These results confirmed that MnO_2 was successfully formed as a result of the redox reactions.

Figure 3 shows the FTIR spectra of AC and AC-Mn. The FTIR spectrum of AC plotted a band at 1575 cm^{-1} which was attributed to the double bond (C═C) vibrations in an aromatic system and the highly conjugated C — O stretching vibration bands [21]. Compared with the FTIR spectrum of AC, liquid-phase

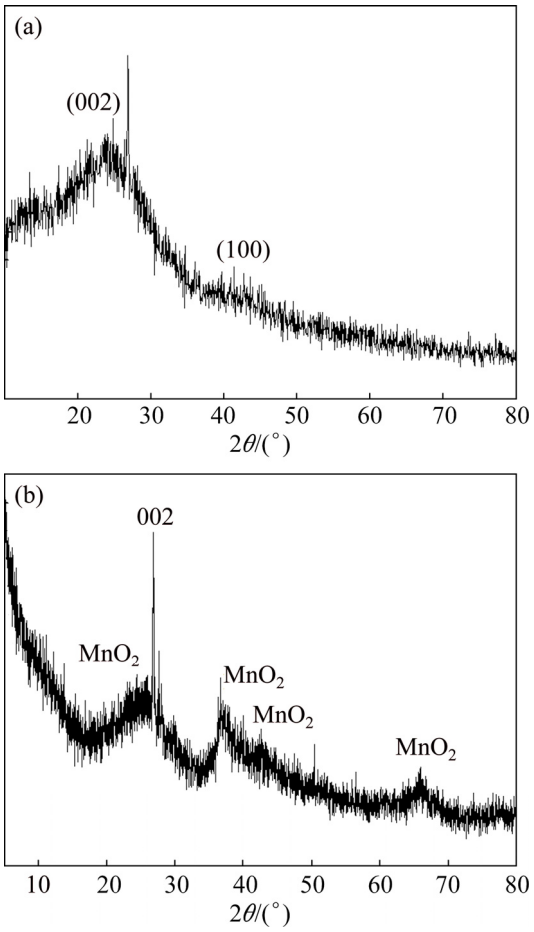

Fig. 2 XRD patterns of AC (a) and AC-Mn (b)

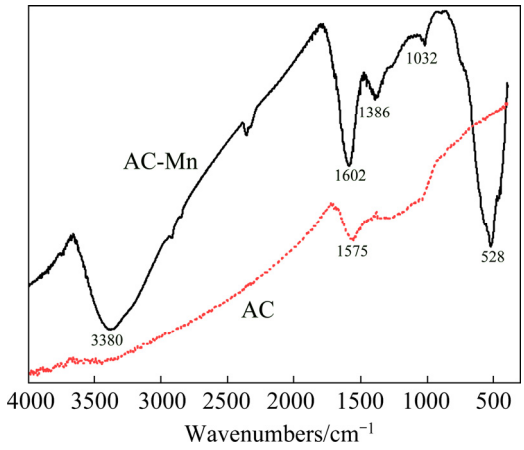

Fig. 3 FTIR spectra of AC and AC-Mn

oxidation modified and produced new IR adsorption peaks. The FTIR spectra of AC-Mn at about 3380, 1386 and 1032 cm^{-1} can be assigned to the —OH stretching vibration, C—C stretch in ring and C—O stretching vibration [19,22], respectively. The peak at 1602 cm^{-1} was the stretching vibrations of COO^-. An obvious change in the spectrum for AC-Mn was the appearance of a new band at 528 cm^{-1}, and these characteristic peaks were ascribed to the Mn—O vibrations [20]. These results suggested that the oxygen-containing functional groups of AC-Mn increased and also confirmed the presence of MnO_2.

Based on this analysis, a simulation scheme was proposed for the illustration of the whole process of AC modification (Scheme 1).

3.2 Results of adsorption experiments

3.2.1 Effect of pH

The influence of the initial pH on the adsorption of Cd^{2+} ions onto AC and AC-Mn is shown in Fig. 4. The removal rate increased with the increase of pH from 3.0 to 4.0, and then the increase slowed down in pH range of 4.0−7.0. The influence of the pH of the solution on the Cd^{2+} ion uptake may be attributed to the fact that at lower pH value, the surfaces of AC and AC-Mn were surrounded by H^+ ions, which prevented Cd^{2+} ions from approaching the binding sites of the adsorbents. The electric repulsion of protons resulted in the suppression of Cd^{2+} adsorption on the adsorbent surface. With increasing pH, the competition from the hydrogen ions decreased and the number of exchangeable binding sites on the surface of adsorbents increased, resulting in the increase in Cd^{2+}adsorption [11,13]. To increase the adsorption capacity and retain the simple form of Cd^{2+} in the solutions, the pH value of 6.0 was selected for the subsequent batch experiments.

3.2.2 Adsorption kinetics

The removal rates of Cd^{2+} adsorbed on AC and AC-Mn at different time are presented in Fig. 5. The removal rate of AC and AC-Mn for Cd^{2+} increased rapidly in the initial stages of contact time and reached equilibrium at 20 min. Afterwards, the removal rate elevated slowly and reached adsorption equilibrium gradually.

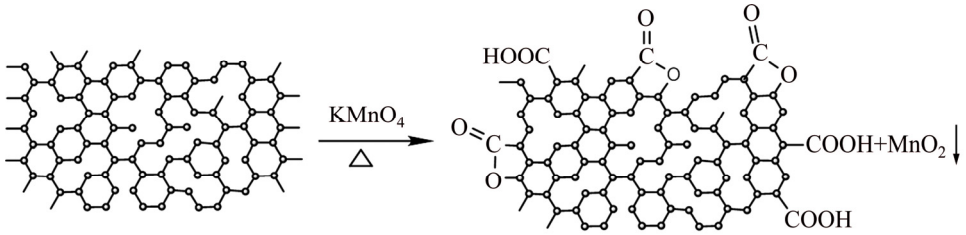

Scheme 1 Schematic for modification of AC

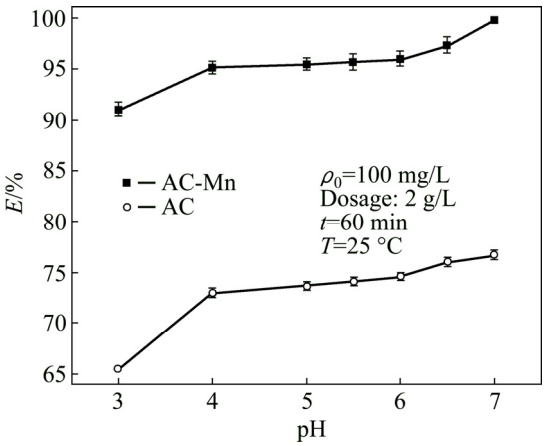

Fig. 4 Effects of pH on removal rate of Cd^{2+} on AC and AC-Mn

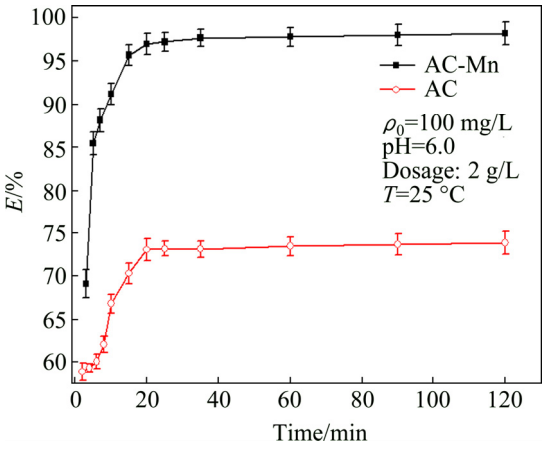

Fig. 5 Effects of contact time on removal rate of Cd^{2+} on AC and AC-Mn

In order to investigate adsorption kinetics of Cd^{2+} on AC and AC-Mn, both pseudo-first order and pseudo-second order kinetic models were used to test the experimental data. The pseudo-first order equation is represented in the form [23]

$$\ln(q_e-q_t)=\ln q_e-k_1t \quad (3)$$

where k_1 is the rate constant of pseudo-first order adsorption, and q_e and q_t denote the amount of adsorption at equilibrium and at time t, respectively.

The pseudo-second order equation is expressed as [24]

$$\frac{t}{q_t}=\frac{1}{k_2q_e^2}+\frac{t}{q_e} \quad (4)$$

where k_2 is the pseudo-second order rate constant. The product $k_2q_e^2$ is actually the initial sorption rate represented as $h=k_2q_e^2$.

The kinetic parameters were calculated using Eqs. (3) and (4) and are provided in Table 2. The initial adsorption rate (h) of AC-Mn was significantly larger than that of AC, indicating that the removal rate of the former was faster than that of the latter. The correlation coefficient (R^2) for pseudo-second order kinetic model was much closer to 1 than that of the first-order kinetic model, and the adsorption capacities calculated by the second-order model were closer to the experimental results. Therefore, the adsorption of Cd^{2+} on AC and AC-Mn was effectively described by the pseudo-second order kinetic model, and successful fitting of the pseudo-second order model indicated that chemical adsorption is the rate-controlling step [25].

3.2.3 Adsorption isotherms

The adsorption isotherms of Cd^{2+} on AC and AC-Mn are shown in Fig. 6. Compared with AC, AC-Mn had higher adsorption capacity for Cd^{2+} because of its more numerous oxygen-containing functional groups, and the generation of MnO_2 increased the adsorption capacity of AC-Mn. MnO_2 has a high affinity for many heavy metals, which can be adsorbed as an inner sphere complex by means of surface complexation on MnO_2 [26]. In the last decade, using MnO_2 as adsorbent for the removal of various heavy metals ions has been attracting attention [26−28].

The experimental data of equilibrium isotherm for Cd^{2+} on AC and AC-Mn were analyzed with Freundlich (Eq. (5)) [29] and Langmuir (Eq. (6)) isotherms [30]:

$$\ln q_e=\ln K_F+\frac{1}{n}\ln \rho_e \quad (5)$$

$$\frac{\rho_e}{q_e}=\frac{1}{q_mb}+\frac{\rho_e}{q_m} \quad (6)$$

where ρ_e (mg/L) is the equilibrium concentration of Cd^{2+} ions, q_e (mg/g) is the amount of Cd^{2+} ions adsorbed at equilibrium, q_m (mg/g) is the maximum adsorption capacity of Cd^{2+} ions, b (L/mg) is the Langmuir isotherm coefficient, and K_F (mg/g) and n are the Freundlich constants.

The parameters of the isotherm models determined from the regression analysis of experimental data are summarized in Table 3. These results indicated that the Langmuir isotherm fitted better than the Freundlich

Table 2 Kinetic parameters for adsorption of Cd^{2+} on AC and AC-Mn

Adsorbent	$q_{e,exp}$/ (mg·g^{-1})	Pseudo-first-order			Pseudo-second-order			
		q_e/ (mg·g^{-1})	k_1/ (L·min^{-1})	R^2	q_e/ (mg·g^{-1})	k_2/ (g·mg^{-1}·min^{-1})	h/ (mg·g^{-1}·min^{-1})	R^2
AC-Mn	49.11	5.37	0.060	0.8671	49.46	0.028	68.967	0.9999
AC	36.95	5.30	0.059	0.8714	37.29	0.029	40.161	0.9998

Table 3 Langmuir and Freundlich parameters for adsorption of Cd^{2+} on AC and AC-Mn

Adsorbent	Langmuir model			Freundlich model		
	q_m/(mg·g^{-1})	b/(L·mg^{-1})	R^2	K_F/(mg·g^{-1})	n	R^2
AC-Mn	217.86	0.018	0.9784	24.29	2.807	0.9481
AC	116.96	0.012	0.9754	12.31	2.924	0.8955

Table 4 Maximum adsorption capacities for Cd^{2+} by various activated carbons

Adsorbent	q/(mg·g^{-1})	Experimental condition		Source
		pH	Adsorbent dosage/(g·L^{-1})	
Activated carbon from olive stone waste residue	7.80	5.0	4	Ref. [8]
Activated carbon from Diplotaxis harra	31.60	6.5	1	Ref. [31]
Activated carbon from aguaje (*Mauritia flexuosa*)	26.33	2.0	0.75	Ref. [32]
Activated carbon from Garcinia mangostana shell	35.97	6.0	0.5	Ref. [21]
Granular AC supported magnesium hydroxide	8.08	6.0	3	Ref. [33]
AC	116.96	6.0	2	Present work
AC-Mn	217.86	6.0	2	Present work

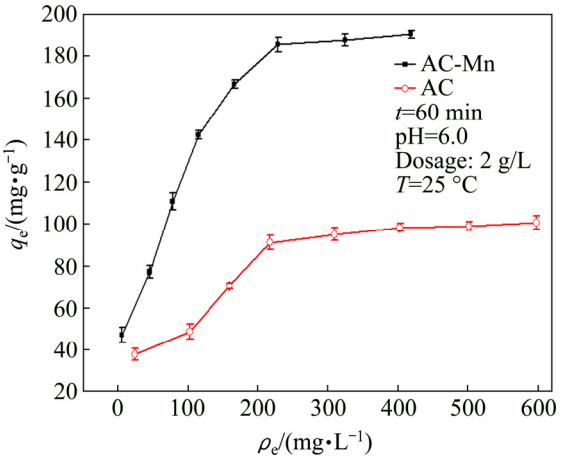

Fig. 6 Adsorption isotherms of Cd^{2+} on AC and AC-Mn

isotherm within the concentration range of research. According to the Langmuir isotherm, the maximum adsorption capacities of AC and AC-Mn for Cd^{2+} were 116.96 and 217.86 mg/g, respectively, which were much higher than those of AC prepared from other raw materials and commercial AC (Table 4).

4 Conclusions

1) *Astragalus* residue was used as a precursor for the preparation of AC, and then AC was modified by $KMnO_4$. AC had great BET surface area and porous honeycomb structure. AC-Mn from *Astragalus* residue loaded a large amount of MnO_2, produced more oxygen-containing functional groups on the basis of AC, and had lower BET surface area than AC.

2) AC and AC-Mn were used to adsorb Cd^{2+} in simulated waste water. The adsorption capacity of AC-Mn for Cd^{2+} increased and became 1.86 times that of AC because of the increase in its oxygen-containing functional groups and the emergence of MnO_2 imparted onto AC by modification. The equilibrium data of Cd^{2+} on AC and AC-Mn were best fitted to Langmuir isotherm. The adsorption process was found to follow the pseudo-second order kinetic model.

3) AC and AC-Mn were employed as a cheap and effective adsorbent for the removal of Cd^{2+} from aqueous solutions because of their cost effectiveness and high adsorption capacities.

References

[1] CHAI Li-yuan, CHEN Yun-nen, SHU Yu-de, CHANG Hao, LI Qing-zhu. Adsorption and removal of cadmium(II) from aqueous solutions by bio-formulation [J]. Transactions of Nonferrous Metals Society of China, 2007, 17: 1057−1062.

[2] BIAN Yu, BIAN Zhao-yong, ZHANG Jun-xiao, DING Ai-zhong, LIU Shao-lei, ZHENG Lei, WANG Hui. Adsorption of cadmium ions from aqueous solutions by activated carbon with oxygen-containing functional groups [J]. Chinese Journal of Chemical Engineering, 2015, 23: 1705−1711.

[3] ZEWAIL T M, YOUSRF N S. Kinetic study of heavy metal ions removal by ion exchange in batch conical air spouted bed [J]. Alexandria Engineering Journal, 2015, 54: 83−90.

[4] SIS H, UYSAL T. Removal of heavy metal ions from aqueous medium using Kuluncak (Malatya) vermiculites and effect of precipitation on removal [J]. Applied Clay Science, 2014, 95: 1−8.

[5] LI Peng, AILIJIANG N, CAO Xiao-xin, LEI Ting, LIANG Peng, ZHANG Xiao-yuan, HUANG Xia, TENG Ji-lin. Pretreatment of coal gasification wastewater by adsorption using activated carbons and activated coke [J]. Colloids and Surfaces A: Physicochemical and

Engineering Aspects, 2015, 482: 177−183.

[6] HEIBATI B, RODRIGUEZ-COUTO S, AL-GHOUTI M A, ASIF M, TYAGI I, AGARWAL S, GUPTA V K. Kinetics and thermodynamics of enhanced adsorption of the dye AR 18 using activated carbons prepared from walnut and poplar woods [J]. Journal of Molecular Liquids, 2015, 208: 99−105.

[7] MONSER L, ADHOUM N. Modified activated carbon for the removal of copper, zinc, chromium and cyanide from wastewater [J]. Separation and Purification Technology, 2002, 26: 137−146.

[8] ALSLAIBI T M, ABUSTAN I, AHMAD M A, FOUL A A. Preparation of activated carbon from olive stone waste: Optimization study on the removal of Cu^{2+}, Cd^{2+}, Ni^{2+}, Pb^{2+}, Fe^{2+}, and Zn^{2+} from aqueous solution using response surface methodology [J]. Journal of Dispersion Science and Technology, 2014, 35: 913−925.

[9] DEMIRAL H, GUNGOR C. Adsorption of copper(II) from aqueous solutions on activated carbon prepared from grape bagasse [J]. Journal of Cleaner Production, 2016, 124: 103−113.

[10] SONG Xiao-lan, LIU Hong-yan, CHENG Lei, QU Yi-xin. Surface modification of coconut-based activated carbon by liquid-phase oxidation and its effects on lead ion adsorption [J]. Desalination, 2010, 255: 78−83.

[11] WANG Yin, WANG Xue-jiang, WANG Xin, LIU Mian, YANG Lian-zhen, WU Zhen, XIA Si-qing, ZHAO Jian-fu. Adsorption of Pb(II) in aqueous solutions by bamboo charcoal modified with $KMnO_4$ via microwave irradiation [J]. Colloids and Surfaces A: Physicochemical and Engineering Aspects, 2012, 414: 1−8.

[12] ELABD H, WANG Han-ping, SHAHEEN A, YAO Hong, ABBASS A. Feeding Glycyrrhiza glabra (liquorice) and Astragalus membranaceus (AM) alters innate immune and physiological responses in yellow perch (Perca flavescens) [J]. Fish & Shellfish Immunology, 2016, 54: 374−384.

[13] MA Chun-fang, FAN Wei, ZHANG Jin-bao, SHI Yang, FENG Ning-chuan. Study of Pb^{2+}, Cd^{2+} and Ni^{2+} adsorption onto activated carbons prepared from glycyrrhiza residue by KOH or H_3PO_4 activation [J]. Water Science and Technology, 2015, 72: 451−462.

[14] BOEHM H P. Some aspects of the surface chemistry of carbon blacks and other carbons [J]. Carbon, 1994, 32: 759−769.

[15] AN Feng-hua, CHENG Yuan-ping, WU Dong-mei, WANG Liang. The effect of small micropores on methane adsorption of coals from Northern China [J]. Adsorption, 2013, 19: 83−90.

[16] CEYHAN A A, ŞAHIN Ö, BAYTAR O, SAKA C. Surface and porous characterization of activated carbon prepared from pyrolysis of biomass by two-stage procedure at low activation temperature and it's the adsorption of iodine [J]. Journal of Analytical and Applied Pyrolysis, 2013, 104: 378−383.

[17] VALLE-VIGON P, SEVILLA M, FUERTES A B. Carboxyl-functionalized mesoporous silica–carbon composites as highly efficient adsorbents in liquid phase [J]. Microporous and Mesoporous Materials, 2013, 176: 78−85.

[18] LU An-hui, ZHENG Jing-tang. Study of microstructure of high-surface-area polyacrylonitrile activated carbon fibers [J]. Journal of Colloid and Interface Science, 2001, 236: 369−374.

[19] XIAO Yong, LONG Cao, ZHENG Ming-tao, DONG Han-wu, LEI Bing-fu, ZHANG Hao-ran, LIU Ying-liang. High-capacity porous carbons prepared by KOH activation of activated carbon for supercapacitors [J]. Chinese Chemical Letters, 2014, 25: 865−868.

[20] PAN Ning, LI Long, DING Jie, LI Sheng-ke, WANG Rui-bing, JIN Yong-dong, WANG Xiang-ke, XIA Chuan-qin. Preparation of graphene oxide-manganese dioxide for highly efficient adsorption and separation of Th(IV)/U(VI) [J]. Journal of Hazardous Materials, 2016, 309: 107−115.

[21] KANG Y L, POON M Y, MONASH P, IBRAHIM S, SARAVANAN P. Surface chemistry and adsorption mechanism of cadmium ion on activated carbon derived from Garcinia mangostana shell [J]. Korean Journal of Chemical Engineering, 2013, 30: 1904−1910.

[22] KARMACHARYA M S, GUPTA V K, TYAGI I.; AGARWAL S, JHA V K. Removal of As(III) and As(V) using rubber tire derived activated carbon modified with alumina composite [J]. Journal of Molecular Liquids, 2016, 216: 836−844.

[23] HAMEED B H, AHMAD A A, AZIZ N. Isotherms, kinetics and thermodynamics of acid dye adsorption on activated palm ash [J]. Chemical Engineering Journal, 2007, 133: 195−203.

[24] HO Y S, MCKAY G. Sorption of copper(II) from aqueous solution by peat [J]. Water Air and Soil Pollution, 2004, 158: 77−97.

[25] FAGHIHIAN H, FARSANI S N. Modification of polyacrylamide–*β*–zeolite composite by phytic acid for the removal of lead from aqueous solutions [J]. Polish Journal of Chemical Technology, 2013, 15: 1−6.

[26] DONG Li-jing, ZHU Zhi-liang, MA Hong-mei, QIU Yan-ling, ZHAO Jian-fu. Simultaneous adsorption of lead and cadmium on MnO_2-loaded resin [J]. Journal of Environmental Sciences, 2010, 22: 225−229.

[27] GHEJU M, BALCU I, MOSOARCH G. Removal of Cr(VI) from aqueous solutions by adsorption on MnO_2 [J]. Journal of Hazardous Materials, 2016, 310: 270−277.

[28] WANG Zi-meng, LEE S W, CATALANO J G, LEZAMA-PACHECO J S, BARGAR J R, TEBO B M, GIAMMAR D E. Adsorption of uranium(VI) to manganese oxides: X-ray absorption spectroscopy and surface complexation modeling [J]. Environmental Science & Technology, 2013, 47: 850−858.

[29] FREUNDLICH H M F. Over the adsorption in solution [J]. Journal of Physical Chemistry, 1906, 57: 385−471.

[30] ALLEN S J, BROWN P A. Isotherm analyses for single component and multi-component metal sorption onto lignite [J]. Journal of Chemical Technology and Biotechnology, 1995, 62: 17−24.

[31] DONG Li-jing, ZHU Zhi-liang, MA Hong-mei, QIU Yan-ling, ZHAO Jian-fu. Simultaneous adsorption of lead and cadmium on MnO_2-loaded resin [J]. Journal of Environmental Sciences, 2010, 22: 225−229.

[32] OBREGON-VALENCIA D, SUN-KOU M D R. Comparative cadmium adsorption study on activated carbon prepared from aguaje (*Mauritia flexuosa*) and olive fruit stones (*Olea europaea L.*) [J]. Journal of Environmental Chemical Engineering, 2014, 2: 2280−2288.

[33] WANG Kang, ZHAO Jian-hai, LI Hai-yan, ZHANG Xin-yu, SHI Huan-huan. Removal of cadmium(II) from aqueous solution by granular activated carbon supported magnesium hydroxide [J]. Journal of the Taiwan Institute of Chemical Engineers, 2016, 61: 287−291.

高锰酸钾改性黄芪废渣活性炭对 Cd^{2+}的吸附

冯宁川[1]，范 玮[1]，朱美霖[1]，郭学益[2]

1. 宁夏医科大学 基础医学院，银川 750004；
2. 中南大学 冶金与环境学院，长沙 410083

摘 要：以黄芪废渣为原料，用 KOH 为活化剂制备黄芪废渣活性炭，并用 $KMnO_4$ 改性，改性前后的黄芪废渣活性炭用于对水溶液中 Cd^{2+}的吸附。采用扫描电子显微术、比表面积测定、X 射线衍射、红外光谱和贝母滴定等方法对改性前后的黄芪废渣活性炭进行表征；通过静态吸附实验考察改性前后黄芪废渣活性炭对水溶液中 Cd^{2+}的吸附性能。结果表明，$KMnO_4$ 改性后活性炭表面含氧官能团增加，MnO_2 沉积到活性炭表面。改性前后的黄芪废渣活性炭对 Cd^{2+}的吸附符合准二级动力学方程，等温吸附更符合 Langmuir 模型，改性前后的黄芪废渣活性炭对 Cd^{2+}的饱和吸附量分别是 116.96 和 217.00 mg/g。$KMnO_4$ 显著改变了黄芪废渣活性炭的物理化学性质和表面结构，改性后的黄芪废渣活性炭对 Cd^{2+}的吸附能力明显提高。

关键词：黄芪废渣；活性炭；改性；吸附；Cd^{2+}

(Edited by Bing YANG)